

**PHS PUBLIC ACCESS**

Author manuscript

*Eurograph IEEE VGTC Symp Vis.* Author manuscript; available in PMC 2015 June 16.

Published in final edited form as:

*Eurograph IEEE VGTC Symp Vis.* 2012 ; 2012: 78–83. doi:10.2312/PE/EuroVisShort/  
EuroVisShort2012/078-083.**Pattern Visualization of Human Connectome Data****Yishi Guo**<sup>1,2,3</sup>, **Yang Wang**<sup>1</sup>, **Shiaofen Fang**<sup>2</sup>, **Hongyang Chao**<sup>3</sup>, **Andrew J. Saykin**<sup>1</sup>, and **Li Shen**<sup>†,1,2</sup><sup>1</sup>Radiology and Imaging Sciences, Indiana University School of Medicine, 950 W Walnut St R2 E124, Indianapolis, IN 46202, USA<sup>2</sup>Computer and Information Science, Purdue University School of Science, 723 W. Michigan St SL280, Indianapolis, IN 46202, USA<sup>3</sup>School of Software, Sun Yat-Sen University, 132 Waihuandong Road, Guangzhou, Guangdong 510006, China**Abstract**

The human brain is a complex network with countless connected neurons, and can be described as a “connectome”. Existing studies on analyzing human connectome data are primarily focused on characterizing the brain networks with a small number of easily computable measures that may be inadequate for revealing complex relationship between brain function and its structural substrate. To facilitate large-scale connectomic analysis, in this paper, we propose a powerful and flexible volume rendering scheme to effectively visualize and interactively explore thousands of network measures in the context of brain anatomy, and to aid pattern discovery. We demonstrate the effectiveness of the proposed scheme by applying it to a real connectome data set.

**1. Introduction**

Recent advances in acquiring multi-modal neuroimaging data provide exciting new opportunities to study how the human brain is wired and how its function is affected by the connectivity pattern. Research in this emerging field, known as *human connectomics* [BSs], holds great promise for a systematic characterization of human brain connectivity and its relationship to cognition and behavior. The human brain is a complex network of approximately  $10^{10}$  neurons linked by  $10^{14}$  synaptic connections [Wik]. Given such an unprecedented complexity, we are facing critical computational challenges for comprehensive mapping and analysis of brain connectivity, across all scales, from the micro-scale of individual synaptic connections between neurons to the macro-scale of brain regions and interregional pathways.

A large body of research has been devoted to extracting brain networks from structural, functional and diffusion magnetic resonance imaging (MRI) data [AB07, BBD\*11, BSs, BS09, RS10, Spo11, CWS\*12, FCD\*08, GWK\*10, HCG\*08, HKG\*07, HSM\*10, MHO\*11, CC11, CGM\*12]. The number of nodes in these networks varies from a few

---

© The Eurographics Association 2012.

<sup>†</sup>Correspondence to shenli@iupui.edu.

dozen to several thousand. Existing studies on analyzing these networks are primarily focused on characterizing them with a small number of easily computable measures that may be inadequate for revealing complex relationship between brain function and its structural substrate. To facilitate large-scale connectomic analysis, we propose a flexible volume rendering scheme to effectively visualize and interactively explore thousands of brain network measures, and to aid pattern discovery. We demonstrate the effectiveness of the proposed scheme by applying it to a real connectome data set.

Volume rendering supports the direct display of volume data sets through semi-transparent images and transfer functions. To highlight segmented volumes or multiple overlapping volumetric fields, existing methods typically modify traditional rendering procedure to traverse multiple segmented data sets. For example, in [HBH03], the segmented components are combined within each cutting slice in a 3D texture mapping algorithm. In [BA02] and [TSH98], a ray casting algorithm is modified to access boundaries of segmented objects during the ray casting process. In [CS01], the intermixing of multiple volumes are assessed at intensity level, opacity level and illumination parameter level at different stages of the rendering process. In our volume rendering algorithm, we apply a unique transfer function based volume intermixing by encoding the multiple volume intensity values within the same volume such that the transfer function can directly access the intermixing information. Since transfer function can be changed dynamically, this approach is more flexible in generating different visual effects interactively by simply manipulating the transfer functions.

## 2. Creation of Structural Connectivity Networks

The topological representation of a network is a collection of nodes and edges between pairs of nodes. Nodes and edges are defined and further combined to construct the brain network. Fig. 1 summarizes the methodology employed in this work for constructing structural connectivity network based on MRI and diffusion tensor imaging (DTI) data. The processing pipeline is divided into three major steps as follows.

1) ROI Generation: Anatomical parcellation is performed using FreeSurfer 5.1 (<http://surfer.nmr.mgh.harvard.edu/>) [FSD99, DFS99, FSB\*02] on the high-resolution T1-weighted anatomical MRI scan acquired with MP-RAGE sequence. The parcellation is an automated operation on each subject to obtain 68 gyral-based ROIs, with 34 cortical ROIs in each hemisphere. The Lausanne parcellation scheme [HCG\*08] is applied to further subdivide these ROIs into smaller ROIs, so that brain networks at different scales (e.g.,  $N_{roi} = 83, 129, 234, 463, \text{ or } 1015$  ROIs/nodes) can be constructed. The T1-weighted MRI image is registered to the low resolution b0 image of DTI data using the FLIRT tool-box in FSL (<http://www.fmrib.ox.ac.uk/fsl.html>), and the warping parameters are applied to the ROIs so that a new set of ROIs in the DTI image space are created. These new ROIs are used for constructing the structural network.

2) DTI tractography: The DTI data are analyzed using FSL. Preprocessing includes correction for motion and eddy current effects in DTI images. The processed images are then output to Diffusion Toolkit (<http://trackvis.org/>) for fiber tracking, using the streamline tractography algorithm called FACT (fiber assignment by continuous tracking). The FACT

algorithm initializes tracks from many seed points and propagates these tracks along the vector of the largest principle axis within each voxel until certain termination criteria are met. A spline filtering is then applied to smooth the tracks.

3) Network Construction: Nodes and edges are defined from the previous results in constructing the weighted, undirected network. The nodes are chosen to be  $N_{roi}$  ROIs obtained from Lausanne parcellation. The weight of the edge between each pair of nodes is defined as the density of the fibers connecting the pair, which is the number of tracks between two ROIs divided by the mean volume of two ROIs [HKG\*07, CWS\*12]. A fiber is considered to connect two ROIs if and only if its end points fall in two ROIs respectively. The weighted network can be described by a matrix (Fig. 1(c-d)). The rows and columns correspond to the nodes, and the elements of the matrix correspond to the weights.

### 3. Visualization Method

Brain connectivity networks obtained through our pipeline can be further taken into complex network analysis. Network measures, such as node degree, strength and efficiency, can be calculated from individuals or average of a population. Different measures may characterize different aspects of the brain connectivity [RS10]. 3D visualization of this connectivity network can provide valuable insight and better understanding of the brain networks and their functions.

A simple way to visualize ROI measures is through a color lookup table. We assign distinct colors for the ROIs according to their network measurement values (e.g., node degree). This color lookup table will then be used as the transfer function in volume rendering of the brain label image, in which each voxel's intensity is its ROI index. In Fig. 2(a), ROIs with high network measurement values are colored red while those with low values are colored blue.

#### 3.1. Volume rendering with highlights

The rendering of the brain label image does not show the original brain volume, which makes it difficult to interpret and understand the connectome in the context of an individual brain anatomy. To provide the volumetric context for the ROIs, we develop a simple and effective volume rendering technique that can highlight individual spots within the brain volume. This allows us to visualize the ROIs within the original brain volume by highlighting the centroids of the ROIs according to the network measures in real time. Fig. 2(b) shows an example of this highlighted volume rendering.

In this technique, we employ a modified color transfer function to map the ROIs measurement values to given highlight colors at the centroid locations. The challenge is to separate the original brain volume intensities from the ROI measurement values in the color mapping process. We choose to expand the voxel intensity field in the brain volume to allow the encoding of the ROI index values at the ROI centroid locations. This enables the color transfer function to assign highlight colors for each ROI centroid point. The method is carried out in three steps (Fig. 3).

Step 1: Creating color table. The color lookup table is created by assigning desired highlight colors to different ROIs according to their network measurement values (Fig. 3(a)).

Step 2: Expanding voxel cells. The voxel intensity values in the original brain volume are expanded to allow the encoding of both the original intensity values and the ROI index values at the ROI centroid locations (Fig. 3(b)). For example, if the original MRI image uses 12 bits to store each intensity value, we can expand the voxel storage by adding another 12 bits for each voxel to store the ROI index values at the appropriate locations (Fig. 3). This allows the manipulation of the color lookup table to render desired highlight colors for voxels carrying ROI index values at the high bits.

Step 3: Color transfer function. Using the modified color lookup table, a standard volume rendering algorithm is able to render the volume with highlights at the encoded locations (centroids) (Fig. 3(c)). This color transfer function (lookup table) can be changed interactively, enabling the visual exploration of various connectome measures in real time.

### 3.2. Exploratory strategies

Several different strategies may be applied to explore the connectome through volume visualization.

- **Scale:** Using Lausanne parcellation scheme, we generate ROIs in 5 different scales, which contain 83, 129, 234, 463, 1015 ROIs respectively. However, there is no optimal scale for connectome analysis, and the most suitable resolution depends on the application [CGM\*12]. Using our method, users can visualize the connectome at any scale, gain insight of the data, and make appropriate decision.
- **Measurement:** Different network measures (Table 1, [RS10]) present different information about the features of the network. Our method allows users to map any measure to ROIs or network nodes for visual evaluation.
- **ROI Selection:** Users can select a certain set of ROIs (e.g., a hemisphere or the hippocampus) to highlight, making other parts of the brain transparent.
- **Thresholding:** Users can set a threshold value for a certain network measurement. Thus, less significant features will not be rendered.

In short, users can perform visual exploratory analysis of the brain network by varying the above parameters: (1) look at the connectome at different scales, (2) identify interesting measurements, (3) localize ROIs, or (4) adjust the threshold for better visual effects. The goal is to have a better understanding of the data and measures, make visual comparison and evaluation, and determine strategies for further analyses.

## 4. Experimental Results

We implemented the proposed scheme based on the Visualization Toolkit (VTK, <http://www.vtk.org/>). We applied the tool to an ongoing connectome study, where participants included 50 young male adults with no history of neurological and psychiatric disorder. Following the pipeline described in Section 2, we extracted structural networks for all

participants using their MRI and DTI data, and calculated the node measurements shown in Table 1. Below we report several examples of our visualization results.

By using the proposed technique, brain networks can be visualized under different measurements and in different network scales. Fig. 4 shows a panel of different visualization results of a sample brain network by varying the network scale and node measurements. Node degree, strength, and other three measures (Table 1) are compared through all 5 different network scales. From this visualization, users can have an intuitive understanding of their data.

Video 1 is an example demonstration of exploring an individual connectome. It includes the following steps: (1) volume rendering of the brain; (2) rendering network nodes with and without showing the brain volume; (3) adjusting network scales; (4) changing the threshold value for rendering “significant” network measures; (5) rendering the measures on the ROIs with and without showing their centroids (i.e., network nodes); and (6) selecting ROIs to render a user-specified subset of brain regions. This demo shows the effectiveness and flexibility of our scheme for exploring an individual connectome, which can greatly help users gain a better understanding of the data in an intuitive fashion.

Video 2 is a demo on how to compare different individual brain networks and their average. This demo focuses on visualizing local efficiency on all the ROIs, using 8 individual brain networks and their average. It presents an intuitive comparison across individuals by visualizing the network measure one by one. An average pattern of this group is also shown at the end of the video. Using this approach, we can explore the mean and variance of the network measures among a group of subjects.

Video 3 shows a demo on how to compare different measures of an individual brain with a group-level pattern. The group-level pattern shown in this example consists of common connectivity modules identified from 24 individual networks using a Bayesian inference model. The common modules are extracted off-line by analyzing the weighted connectivity matrices [RS10]. Such a visualization facilitates comparison between individual data and group-level pattern as well as comparison between different networks measures of the same individual connectome.

The above results have clearly demonstrated that the proposed method can greatly aid in human connectome research by extracting new insights from complex neuroimaging data. A better understanding of the data could be achieved at the individual level (Video 1), the group level (Video 2), or by comparing different individual measures together with a group level pattern (Video 3). Using the proposed method, we have learned useful patterns which could not be seen before. For example, two functional segregation measures (Table 1), clustering coefficient and local efficiency, have demonstrated similar patterns at all the scales except scale 83 (Fig. 4). Such type of knowledge can help us determine which scale or which measure to focus on in further studies.

## 5. Conclusions

Human connectomics has attracted a lot of recent attention in brain research. As a highly promising new field, it studies the complex architecture of the human brain and its connections in great detail. To facilitate large-scale human connectome analysis, in this paper, we have proposed a powerful and flexible volume rendering scheme to effectively visualize and interactively explore thousands of network measures in the context of brain anatomy, in order to guide subsequent analyses and aid pattern discovery. We have applied our technique to a real connectome data set and presented several examples of visual exploration and comparison of individual brain networks and group-level patterns. The promising results have demonstrated the effectiveness and flexibility of the proposed method. Future research will be very important to incorporate the visualization of network edges and edge properties into this volume rendering scheme to have a complete visual representation of the entire connectome.

## Acknowledgments

Supported by NSF IIS-1117335, NIH UL1 RR025761, U01 AG024904, NIA RC2 AG036535, NIA R01 AG19771, and NIA P30 AG10133-18S1.

## References

- AB07. Achard S, Bullmore E. Efficiency and cost of economical brain functional networks. *PLoS Comput Biol.* 2007; 3(2):e17. 1. [PubMed: 17274684]
- BA02. Bullitt E, Aylward S. Volume rendering of segmented image objects. *IEEE Transaction on Medical Imaging.* 2002; 21(8):998–1002. 1.
- BBD\*11. Bassett DS, Brown JA, Deshpande V, Carlson JM, Grafton ST. Conserved and variable architecture of human white matter connectivity. *Neuroimage.* 2011; 54(2):1262–1279. 1. [PubMed: 20850551]
- BS09. Bullmore E, Sporns O. Complex brain networks: graph theoretical analysis of structural and functional systems. *Nat Rev Neurosci.* 2009; 10(3):186–198. 1. [PubMed: 19190637]
- BSss. Behrens TEJ, Sporns O. Human connectomics. *Current Opinion in Neurobiology.* 2012 in press. 1.
- CC11. Consortium W.-M., Consortium H.-U. The NIH Human Connectome Project. 2011 1.
- CGM\*12. Cammoun L, Gigandet X, Meskaldji D, Thiran JP, Sporns O, Do KQ, Maeder P, Meuli R, Hagmann P. Mapping the human connectome at multiple scales with diffusion spectrum mri. *Journal of Neuroscience Methods.* 2012; 203(2):386–397. 1, 3. [PubMed: 22001222]
- CS01. Cai W, Sakas G. Data intermixing and multi-volume rendering. *Computer Graphics Forum.* 2001; 18(3):359–368. 1.
- CWS\*12. Cheng H, Wang Y, Sheng J, Sporns O, Kronenberger WG, Mathews VP, Hummer TA, Saykin AJ. Optimization of seed density in dti tractography for structural networks. *J Neurosci Methods.* 2012; 203(1):264–72. 1, 2. [PubMed: 21978486]
- DFS99. Dale A, Fischl B, Sereno M. Cortical surface-based analysis. i. segmentation and surface reconstruction. *Neuroimage.* 1999; 9(2):179–94. 2. [PubMed: 9931268]
- FCD\*08. Fair DA, Cohen AL, Dosenbach NUF, Church JA, Miezin FM, Barch DM, Raichle ME, Petersen SE, Schlaggar BL. The maturing architecture of the brain's default network. *Proceedings of the National Academy of Sciences.* 2008; 105(10):4028–4032. 1.
- FSB\*02. Fischl B, Salat DH, Busa E, Albert M, Dieterich M, Haselgrove C, van der Kouwe A, Killiany R, Kennedy D, Klaveness S, Montillo A, Makris N, Rosen B, Dale AM. Whole brain segmentation: automated labeling of neuroanatomical structures in the human brain. *Neuron.* 2002; 33(3):341–55. 2. [PubMed: 11832223]

- FSD99. Fischl B, Sereno M, Dale A. Cortical surface-based analysis. ii: Inflation, flattening, and a surface-based coordinate system. *Neuroimage*. 1999; 9(2):195–207. 2. [PubMed: 9931269]
- GWK\*10. Glahn DC, Winkler AM, Kochunov P, Almasy L, Duggirala R, Carless MA, Curran JC, Olvera RL, Laird AR, Smith SM, Beckmann CF, Fox PT, Blangero J. Genetic control over the resting brain. *Proceedings of the National Academy of Sciences*. 2010; 107(3):1223–1228. 1.
- HBH03. Hadwiger M, Berger C, Hauser H. High-quality two-level volume rendering of segmented data sets on consumer graphics hardware. *IEEE Visualization*. 2003:301–308. 1.
- HCG\*08. Hagmann P, Cammoun L, Gigandet X, Meuli R, Honey CJ, Wedeen VJ, Sporns O. Mapping the structural core of human cerebral cortex. *PLoS Biol*. 2008; 6(7):e159. 1, 2. [PubMed: 18597554]
- HKG\*07. Hagmann P, Kurant M, Gigandet X, Thiran P, Wedeen VJ, Meuli R, Thiran JP. Mapping human whole-brain structural networks with diffusion MRI. *PLoS One*. 2007; 2(7):e597. 1, 2. [PubMed: 17611629]
- HSM\*10. Hagmann P, Sporns O, Madan N, Cammoun L, Pienaar R, Wedeen VJ, Meuli R, Thiran JP, Grant P. White matter maturation reshapes structural connectivity in the late developing human brain. *Proceedings of the National Academy of Sciences*. 2010 1.
- MHO\*11. Marcus DS, Harwell J, Olsen T, Hodge M, Glasser MF, Prior F, Jenkinson M, Laumann T, Curtiss SW, Van Essen DC. Informatics and data mining tools and strategies for the human connectome project. *Front Neuroinform*. 2011; 5:4. 1. [PubMed: 21743807]
- RS10. Rubinov M, Sporns O. Complex network measures of brain connectivity: uses and interpretations. *Neuroimage*. 2010; 52(3):1059–69. 1, 2, 3, 4. [PubMed: 19819337]
- Spo11. Sporns O. The human connectome: a complex network. *Annals of the New York Academy of Sciences*. 2011; 1224(1):109–125. 1. [PubMed: 21251014]
- TSH98. Tiede U, Schiemann T, Hohne K. High quality rendering of attributed volume data. *IEEE Visualization*. 1998:255–262. 1.
- Wik. Wikipedia C. Connectome. Sep 25.2011 20:35. UTC. 1.



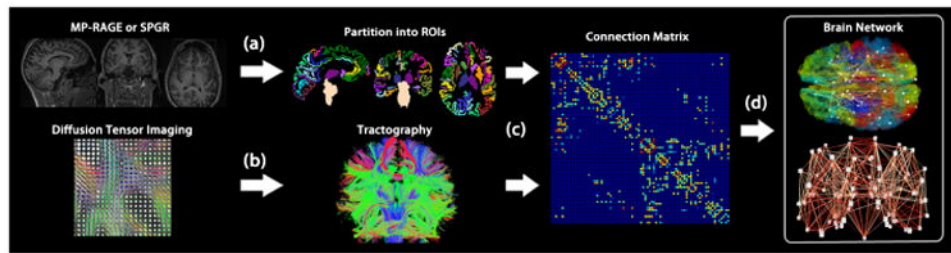


**Figure 1.**

Creation of structural connectivity networks. (a) ROI definition via brain segmentation and cortical parcellation on MP-RAGE or SPGR scan. (b) Fiber extraction via DTI tractography. (c) Creation of connectivity matrix  $M$ , where  $M(i, j)$  stores the connectivity measure (i.e., edge weight) between ROI  $i$  and ROI  $j$ . (d) Visualization of connectivity matrix as brain network.



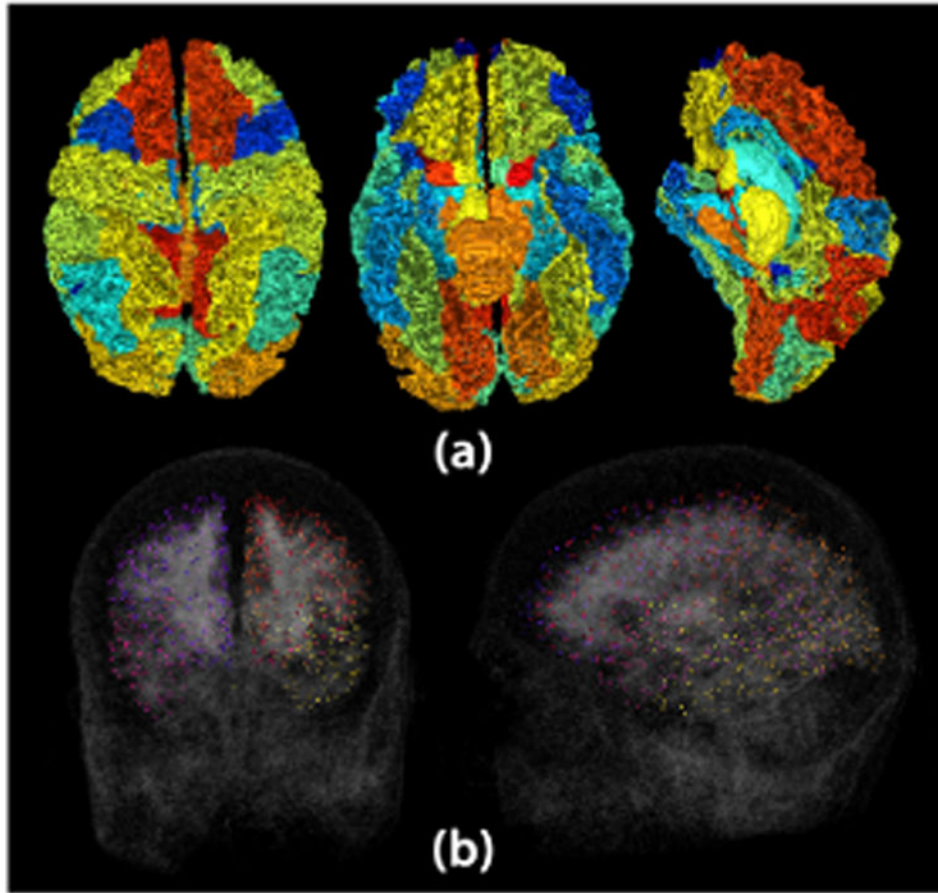


**Figure 2. Connectome visualization: (a) ROI visualization, (b) volume rendering with highlighted nodes**

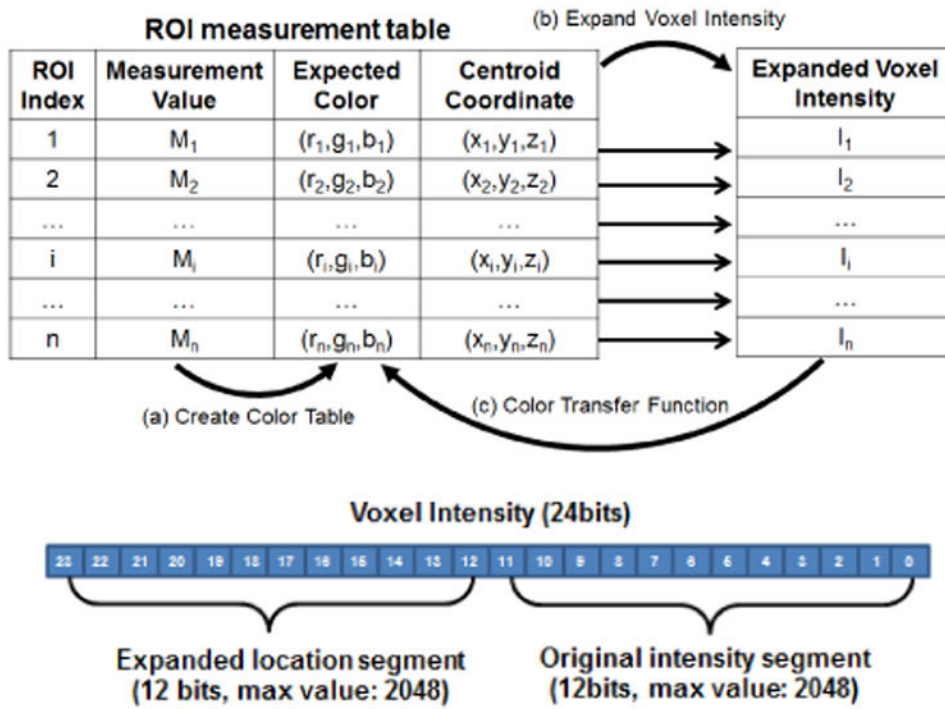


Figure 3. Top panel: offline expanding method for rendering with highlights; bottom panel: expanded voxel intensity

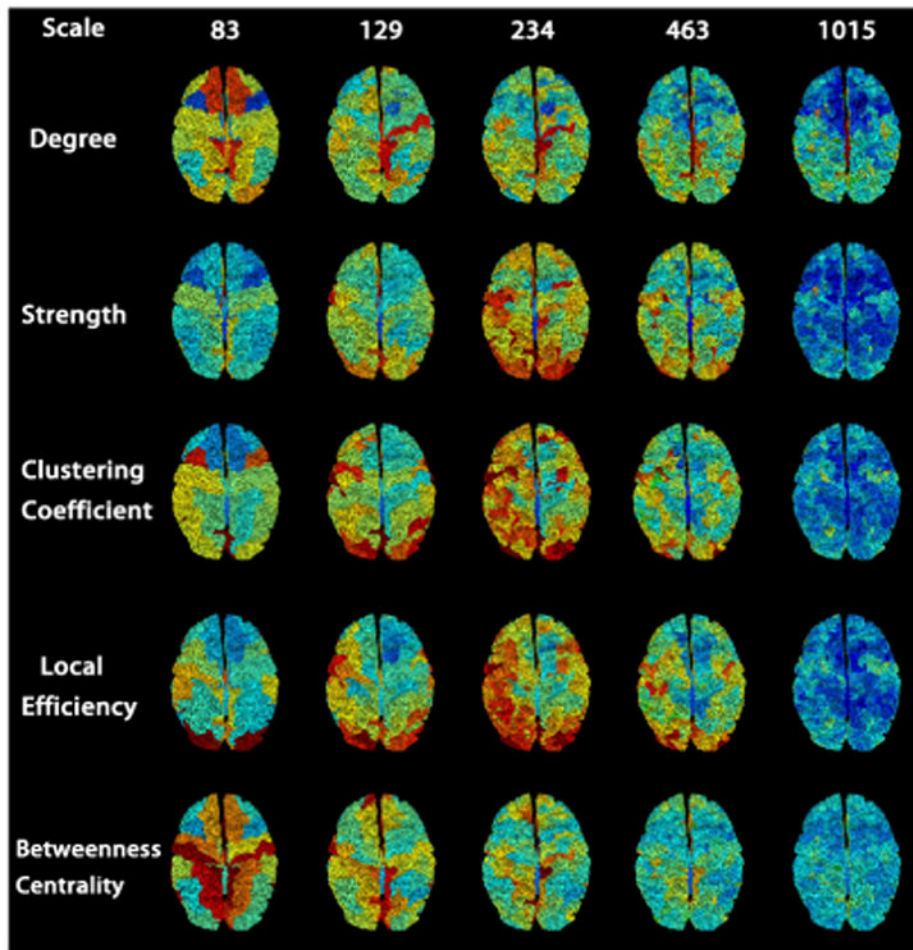


Figure 4. Visual comparison of five network measurements through all scales (Scale ID indicates the number of nodes)

**Table 1**  
**Example measurements of network nodes, see [RS10] for more network measures and their details**

| Name                   | Description   |
|------------------------|---|
| Degree                 | Number of links connected to the node (a basic and important network measure)                               |
| Strength               | Sum of weights of links connected to the node (the weighted variant of the degree)                          |
| Clustering Coefficient | Fraction of triangles around a node (a measure of segregation)  |
| Local Efficiency       | Average of inverse shortest path length computed on the neighborhood of the node (a measure of segregation) |
| Betweenness Centrality | Fraction of all shortest paths in the network that contain a given node (a measure of centrality)           |

Author Manuscript

Author Manuscript

Author Manuscript

Author Manuscript